Journal of Engg. Research **Vol. 5 No. (6) March 2018 pp.** *1-14*

نية

A new control chart using the process loss index function

Ching-Ho Yen*,Muhammad Aslam**, Chia-Hao Chang*** and Chi-Hyuck Jun****

** Department of Industrial Engineering & Management Information, Huafan University, Taipei, Taiwan*

***Department of Statistics, Faculty of Science, King Abdulaziz University, Jeddah 21551, Saudi Arabia.*

Email: aslam_ravian@hotmail.com

****Department of Nursing, Chang Gung Institute of Technology, Chiayi, Taiwan*

*****Department of Industrial and Management Engineering, POSTECH, Pohang 790-784, Republic of Korea*

**Corresponding Author: aslam_ravian@hotmail.com*

Abstract

A control chart is a powerful tool used to monitor the variation of a process. In this paper, a new viewpoint of control chart based on process loss index is proposed. The control limits for chart are constructed. The operating characteristics function of chart is derived, which is used to describe how well the control chart can detect assignable causes. Also an average run length is computed to show how many samples are needed for the control chart to discover a change of process. In addition, comparisons are made with the existing control chart based on Cpm (Spiring, 1995) in terms of the operating characteristic curve and average run length. Finally, a real world example is given to illustrate the proposed methodology. Through the proposed method, practitioners can determine the corresponding sample size based on a desired value of the average run length to make the chart for monitoring the process capability.

Key words: Control chart; process loss index; operating characteristic curve; average run length.

1. Introduction

Statistical process control (SPC) is a methodology that detects whether one process is in control or not based on the information from samples and takes corrective actions if necessary. The objective of SPC is to prevent the production of defective products. The production process may shift due to several reasons such as workers mistakes and machine wear and consequently lead to the increment of the defective products. One of the most important tools for SPC is the control chart. Control charts have many applications in the industries for monitoring the production process. The control charts are used to detect the shift/cause of the variation in the process. During the production process, the mean, variance, or both can shift. Control charts are useful in separating the cause of the variation from the natural variation. Whatever the type of the control chart is, two errors are unavoidable. The probability of declaring, in the control process, whether being out of control process is called type-I error or the false alarm, denoted by α . The probability of inferring that the process is in control when actually it is out of control is called type-II error, denoted by β . So, the efficient control charts can minimize risks and quickly detect changes when the process shifts (Serel, 2009).

Shewhart X-bar control charts are used to monitor the shift in the mean and R and charts are commonly used for the monitoring of the process variation. The monitoring of both quantities separately needs more time, cost, resources, and manpower. Therefore, a control chart that is used to monitor the process mean and variation simultaneously is preferred (Cheng & Thaga, 2006). For more details, the reader may refer to Chen et al. (2004), Costa & Rahim (2006), Wu & Tian (2005), Wu et al. (2005), Zhang & Wu (2006), Wu & Tian (2006), Wu et al. (2009), Hawkins & Deng (2009), Li et al. (2010), Zhang et al. (2010), Khoo et al. (2010a), Khooet et al. (2010b), Zhou et al. (2010), Huang & Chen (2010), Zhang et al. (2011), Ouet al. (2011), Memar & Niaki (2011), Teh et al. (2011), Teh et al.(2012).

It is important to note that, during the manufacturing stage, it may be impossible to produce the product exactly at the target value. The process may deviate due to certain factors. The deviation from the quality variable to its target value is called the loss of the process. The companies want to minimize this loss to get more satisfaction. As Spiring & Yeung (1998) mentioned, the loss function is widely used in industries to measure this deviation. Therefore, the use of the loss function attracts researchers for the development of control charts using it. Recently, Yang (2013) proposed a variable sampling interval (VSI) based on the exponentially weighted moving average (EWMA) using the loss function.

Traditionally, the product manufactured with the given specification limits is considered equally conforming and nonconforming if it is outside the limits. However, this measure does not distinguish between the differences of the products that fall within the specification limits. To remedy this, Johnson (1992) proposed the process loss index L_e for two-sided specification case with normal distribution, to provide numerical measures on the process performance for industrial applications. By exploring the literature, we find that no work based on L_e is proposed.

In this paper, we will present the design of a control chart using the L_e, which considers three cases, that is, (i) mean shift, (ii) variation shift, and (iii) both mean and variation. The rest of the paper is organized as follows. The design of the proposed control chart for the process loss consideration is given in section 2. The performance of the proposed control chart is discussed in section 3. The application of the proposed plan is given in section 4 and the concluding remarks are given in the last section.

2. The Design of Control Chart with Process Loss Consideration

2.1The Process Loss Index

The process loss index L_e is defined as the ratio of the expected quadratic loss and square of half specification width as follows:

$$L_e = \int_{-\infty}^{\infty} \left[\frac{(x-T)^2}{d^2} \right] f(x)\, dx = \frac{\sigma^2 + (\mu - T)^2}{d^2}$$

where *f(x)* is the probability density function of a quality characteristic of interest, is the process mean, is the process standard deviation, *T* is the target value, $d = (USL\text{-}LSL)/2$ is the half specification width, and *USL* and *LSL* are the upper and lower specification limits, respectively.

The advantage of L_e over C_{pm} is that the estimator of the former has better statistical properties than those of the latter, as the former does not involve a reciprocal transformation of process mean and variance. The C_{pm} is defined as

$$C_{pm} = \frac{USL - LSL}{6\sqrt{\sigma^2 + (\mu - T)^2}}$$

In practice, the true value of parameter L_e is usually unknown; the sample data must be collected to estimate parameter L_e . To estimate the process loss index L_e , we consider the natural estimator L_e , the maximum likelihood estimator (MLE) of L_e , defined as follows:

$$\hat{L}_e = \frac{S_n^2}{d^2} + \frac{(\overline{X} - T)^2}{d^2} = \frac{1}{n}\sum_{i=1}^{n}\frac{(X_i - \overline{X})^2}{d^2} + \frac{(\overline{X} - T)^2}{d^2} = \frac{\sum_{i=1}^{n}(X_i - T)^2}{nd^2}$$

where $\overline{X} = \sum_{i=1}^{n} X_i / n$, $S_n^2 = \sum_{i=1}^{n}(X_i - \overline{X})^2 / n$.

Referring to the above definition of equation and the assumption of normal distribution, a mathematical relationship can be expressed as follows:

$$\frac{\hat{L}_e}{L_e} = \frac{\sum_{i=1}^{n}(X_i - T)^2}{nd^2} \times \frac{d^2}{[\sigma^2 + (\mu - T)^2]} = \frac{\dfrac{\sum_{i=1}^{n}(X_i - T)^2}{\sigma^2}}{n[1 + \dfrac{(\mu - T)^2}{\sigma^2}]} = \frac{\chi^2_{n,\delta}}{n + \delta},$$

where $\chi^2_{n,\delta}$ is a non-central Chi-square distribution with n degrees of freedom and non-central parameter $\delta = n(\mu - T)^2 / \sigma^2 = n\varepsilon^2$. The given statistics are different from those of Yang (2013).

2.2 The Control Limits for $\hat{L}_e$ Chart

Given $\hat{L}_e$ is distributed as $L_e\chi^2_{n,\delta} / (n + \delta)$, so we can derive

$$E(\hat{L}_e) = E[L_e\chi^2_{n,\delta} / (n + \delta)] = \frac{L_e}{n + \delta} E(\chi^2_{n,\delta}) = L_e$$

$$Var(\hat{L}_e) = Var[L_e\chi^2_{n,\delta} / (n + \delta)] = L_e^2 \frac{2n + 4\delta}{(n + \delta)^2} = L_e^2 \frac{2n + 4n\varepsilon^2}{n^2(1 + \varepsilon^2)^2}$$

Based on the principle of building control chart with 3-sigma, the control limits for $\hat{L}_e$ chart can be expressed as

$$UCL(\hat{L}_e) = E(\hat{L}_e) + 3\sqrt{Var(\hat{L}_e)} = L_e + 3\sqrt{L_e^2 \frac{2n + 4n\varepsilon^2}{n^2(1 + \varepsilon^2)^2}} = L_e + 3\frac{L_e}{n(1 + \varepsilon^2)}\sqrt{2n + 4n\varepsilon^2}$$

$$CL(\hat{L}_e) = L_e$$

$$LCL(\hat{L}_e) = E(\hat{L}_e) - 3\sqrt{Var(\hat{L}_e)} = L_e - 3\sqrt{L_e^2 \frac{2n + 4n\varepsilon^2}{n^2(1 + \varepsilon^2)^2}} = L_e - 3\frac{L_e}{n(1 + \varepsilon^2)}\sqrt{2n + 4n\varepsilon^2}$$

Because L_e is usually unknown, it should be estimated from m samples from the in-control process. If $\hat{L}_{e_i}$ denotes the estimator at the i-th subgroup, then L_e can be estimated by the sample mean over *m* subgroups.

$$\bar{\hat{L}}_e = \frac{\sum_{i=1}^{m} \hat{L}_{e_i}}{m},$$

where $\hat{L}_{e_i} = \dfrac{S_i^2 + (\bar{X}_i - T)^2}{d^2}$, $S_i^2 = \dfrac{\sum_{j=1}^{n} (X_{ij} - \bar{X}_i)^2}{n}$, $\bar{X}_i = \dfrac{\sum_{j=1}^{n} X_{ij}}{n}$, $i=1,2,\ldots,m$.

Hence, the control limits for $\hat{L}_e$ control chart can be expressed as

$$UCL = \bar{\hat{L}}_e + 3\frac{\bar{\hat{L}}_e}{n(1+\hat{\varepsilon}^2)}\sqrt{2n + 4n\hat{\varepsilon}^2}$$

$$CL = \bar{\hat{L}}_e$$

$$LCL = \bar{\hat{L}}_e - 3\frac{\bar{\hat{L}}_e}{n(1+\hat{\varepsilon}^2)}\sqrt{2n + 4n\hat{\varepsilon}^2},$$

where $\hat{\varepsilon}$ is the estimator of ε by estimating the mean and variance of the process. Note that *LCL* will be set to be 0 if *LCL* is less than 0.

The new control chart based on the process loss function operates as follows at each subgroup over time:

Step-1: Select a random sample of size *n* from the production process. Compute the statistic

$$\hat{L}_e = \frac{\sum_{i=1}^{n} (X_i - T)^2}{nd^2}$$

Step-2: Declare the process as in-control if $LCL \le \hat{L}_e \le UCL$ and without any special pattern; otherwise, declare that the process is out-of-control.

It is noted that the analysis of $\hat{L}_e$ chart should be implemented only when the process is in a state of process in control. For the proposed control chart to be practical and convenient to use, a flowchart is provided below.

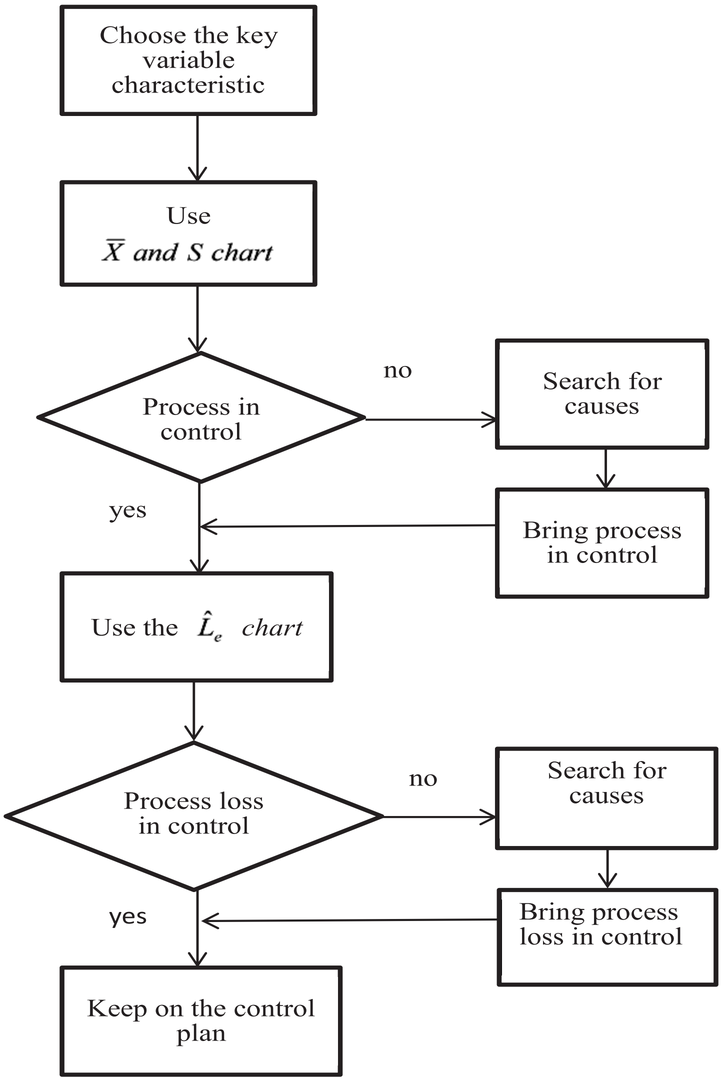

Figure 1. Flowchart for implementing the $\hat{L}_e$ chart.

2.3 OC Function for $\hat{L}_e$ Chart

In this part, we derive the OC function of the control chart based on L_e for three cases, respectively.

Case 1: μ shifts

When the process mean μ moves to a new location $\mu^* = \mu + k\sigma$, the relationship between the new L_e^* and L_e can be expressed as $\frac{L_e^*}{L_e} = \frac{1+\left(\frac{\mu-T}{\sigma}+k\right)^2}{1+\left(\frac{\mu-T}{\sigma}\right)^2} = \frac{1+(\varepsilon+k)^2}{1+\varepsilon^2}$, that is, $L_e^* = L_e\left(\frac{1+(\varepsilon+k)^2}{1+\varepsilon^2}\right)$.

It can be shown that

$$n(1+(\varepsilon+k)^2)\frac{\hat{L}_e}{L_e^*} \sim \chi^2_{n,\delta^*},$$

where $\delta^* = n(\mu + k\sigma - T)^2/\sigma^2 = n(\varepsilon+k)^2$.

So the OC curve for $\hat{L}_e$ chart can be built as

$$\beta(L_e) = P\left(L_e - 3\frac{L_e}{n(1+\varepsilon^2)}\sqrt{2n+4n\varepsilon^2} \le \hat{L}_e \le L_e + 3\frac{L_e}{n(1+\varepsilon^2)}\sqrt{2n+4n\varepsilon^2} \mid \mu^* = \mu + k\sigma\right)$$

$$= P\left(\frac{n(1+(\varepsilon+k)^2)\left(L_e - 3\frac{L_e}{n(1+\varepsilon^2)}\sqrt{2n+4n\varepsilon^2}\right)}{L_e^*} \le n(1+(\varepsilon+k)^2)\frac{\hat{L}_e}{L_e^*} \le \frac{n(1+(\varepsilon+k)^2)\left(L_e + 3\frac{L_e}{n(1+\varepsilon^2)}\sqrt{2n+4n\varepsilon^2}\right)}{L_e^*}\right)$$

$$= P\left(n(1+\varepsilon^2) - 3\sqrt{2n+4n\varepsilon^2} \le \chi^2_{n,\delta^*} \le n(1+\varepsilon^2) + 3\sqrt{2n+4n\varepsilon^2}\right) \tag{1}$$

Similarly, when the process mean μ shifts to $\mu^* = \mu - k\sigma$, the OC curve for $\hat{L}_e$ chart can be built as

$$\beta(L_e) = P\left(n(1+\varepsilon^2) - 3\sqrt{2n+4n\varepsilon^2} \le \chi^2_{n,\delta^*} \le n(1+\varepsilon^2) + 3\sqrt{2n+4n\varepsilon^2}\right)$$

where $\delta^* = n(\mu - k\sigma - T)^2/\sigma^2 = n(\varepsilon - k)^2$ (2)

Case 2: σ changes

When the process standard deviationchanges into a new scale $\sigma^* = r\sigma$, the relationship between the new L_e^* and L_e can be expressed as $\frac{L_e^*}{L_e} = \frac{1+\left(\frac{\mu-T}{r\sigma}\right)^2}{(1/r)^2 + \left(\frac{\mu-T}{r\sigma}\right)^2} = \frac{1+(\varepsilon/r)^2}{(1/r)^2+(\varepsilon/r)^2}$

that is, $L_e^* = L_e\left(\frac{1+(\varepsilon/r)^2}{(1/r)^2+(\varepsilon/r)^2}\right)$.

It can be shown that

$$n\left(1+(\varepsilon/r)^2\right)\frac{\hat{L}_e}{L_e^*} \sim \chi^2_{n,\delta^*},$$

where $\delta^* = n(\mu - T)^2/(r\sigma)^2 = n(\varepsilon/r)^2$.

So the OC curve for $\hat{L}_e$ chart can be built as

$$\beta(L_e) = P\left(L_e - 3\frac{L_e}{n(1+\varepsilon^2)}\sqrt{2n+4n\varepsilon^2} \le \hat{L}_e \le L_e + 3\frac{L_e}{n(1+\varepsilon^2)}\sqrt{2n+4n\varepsilon^2} \mid \sigma^* = r\sigma\right)$$

$$= P\left(\frac{n\left(1+(\varepsilon/r)^2\right)\left(L_e - 3\frac{L_e}{n(1+\varepsilon^2)}\sqrt{2n+4n\varepsilon^2}\right)}{L_e^*} \le n\left(1+(\varepsilon/r)^2\right)\frac{\hat{L}_e}{L_e^*} \le \frac{n\left(1+(\varepsilon/r)^2\right)\left(L_e + 3\frac{L_e}{n(1+\varepsilon^2)}\sqrt{2n+4n\varepsilon^2}\right)}{L_e^*}\right)$$

$$= P\left(n\left(1/r^2 + \varepsilon^2/r^2\right) - 3\left(\frac{1/r^2 + \varepsilon^2/r^2}{1+\varepsilon^2}\right)\sqrt{2n+4n\varepsilon^2} \le \chi^2_{n,\delta^*} \le n\left(1/r^2 + \varepsilon^2/r^2\right) + 3\left(\frac{1/r^2 + \varepsilon^2/r^2}{1+\varepsilon^2}\right)\sqrt{2n+4n\varepsilon^2}\right) \tag{3}$$

Case 3: μ shifts and σ changes simultaneously

When the process mean μ moves to a new location $\mu^* = \mu + k\sigma$ and the process standard deviation σ changes into $\sigma^* = r\sigma$, the relationship between the new L_e^* and L_e can be expressed as $\frac{L_e^*}{L_e} = \frac{1+\left(\frac{\mu + k\sigma - T}{r\sigma}\right)^2}{(1/r)^2 + \left(\frac{\mu - T}{r\sigma}\right)^2} = \frac{1+(\varepsilon/r + k/r)^2}{(1/r)^2 + (\varepsilon/r)^2}$, that is, $L_e^* = L_e\left(\frac{1+(\varepsilon/r + k/r)^2}{(1/r)^2 + (\varepsilon/r)^2}\right)$.

It can be shown that

$$n\left(1+(\varepsilon/r + k/r)^2\right)\frac{\hat{L}_e}{L_e^*} \sim \chi^2_{n,\delta^*}$$

where $\delta^* = n(\mu + k\sigma - T)^2/(r\sigma)^2 = n(\varepsilon/r + k/r)^2$.

So the OC curve for $\hat{L}_e$ chart can be built as

$$\beta(L_e) = P\left(L_e - 3\frac{L_e}{n(1+\varepsilon^2)}\sqrt{2n+4n\varepsilon^2} \le \hat{L}_e \le L_e + 3\frac{L_e}{n(1+\varepsilon^2)}\sqrt{2n+4n\varepsilon^2} \mid \sigma^* = r\sigma\right)$$

$$= P\left(\frac{n\left(1+(\varepsilon/r + k/r)^2\right)\left(L_e - 3\frac{L_e}{n(1+\varepsilon^2)}\sqrt{2n+4n\varepsilon^2}\right)}{L_e^*} \le n\left(1+(\varepsilon/r + k/r)^2\right)\frac{\hat{L}_e}{L_e^*} \le \frac{n\left(1+(\varepsilon/r + k/r)^2\right)\left(L_e + 3\frac{L_e}{n(1+\varepsilon^2)}\sqrt{2n+4n\varepsilon^2}\right)}{L_e^*}\right)$$

$$P\left(n\left(1/r^2 + \varepsilon^2/r^2\right) - 3\left(\frac{1/r^2 + \varepsilon^2/r^2}{1+\varepsilon^2}\right)\sqrt{2n+4n\varepsilon^2} \le \chi^2_{n,\delta^*} \le n\left(1/r^2 + \varepsilon^2/r^2\right) + 3\left(\frac{1/r^2 + \varepsilon^2/r^2}{1+\varepsilon^2}\right)\sqrt{2n+4n\varepsilon^2}\right) \tag{4}$$

Similarly, when the process mean μ moves to a new location $\mu^* = \mu - k\sigma$ and the process standard deviation σ changes into $\sigma^* = r\sigma$, the OC curve for $\hat{L}_e$ chart can be built as

$$P\left(n\left(1/r^2+\varepsilon^2/r^2\right)-3\left(\frac{1/r^2+\varepsilon^2/r^2}{1+\varepsilon^2}\right)\sqrt{2n+4n\varepsilon^2}\le \chi^2_{n,\delta^*}\le n\left(1/r^2+\varepsilon^2/r^2\right)+3\left(\frac{1/r^2+\varepsilon^2/r^2}{1+\varepsilon^2}\right)\sqrt{2n+4n\varepsilon^2}\right) \quad (5)$$

where $\delta^* = n(\mu-k\sigma-T)^2/(r\sigma)^2 = n(\varepsilon/r-k/r)^2$

In fact, ε is usually unknown, so we execute the sensitivity analysis that examines the behavior of ε against the probability of 3-sigma control limits to find the suitable value of ε. Figure 2 displays the probability 1- α of falling within the control limits versus the ε value for n=4, 6, 8, 10, 12. From Figure 2, we can observe that probability 1- α will be smallest at ε =0 for all n values. For a specified n, the control limits with the smallest value of 1- α can be regarded as the optimal control limits, which leads to the smallest probability of β that does not detect changes when the process is out of control. Therefore, for practical purposes, we can use ε =0 to calculate 3-sigma control limits of $\hat{L}_e$ without having to estimate the parameter ε. In order to evaluate the suitability for 3-Sigma control limit of the control chart we proposed, we use the Western Electronic Rules to verify it. Table 1 displays the probabilities that fall into every region within the 3-sigma control limit and fall out of the 3-sigma control limit for the $\hat{L}_e$ control chart. Table 2 displays the corresponding probabilities for each one in Western Electronic Rules, which shows that the probability for each rule is very small. Therefore, we can conclude that the use of the 3-sigma control limit of the control chart is suitable.

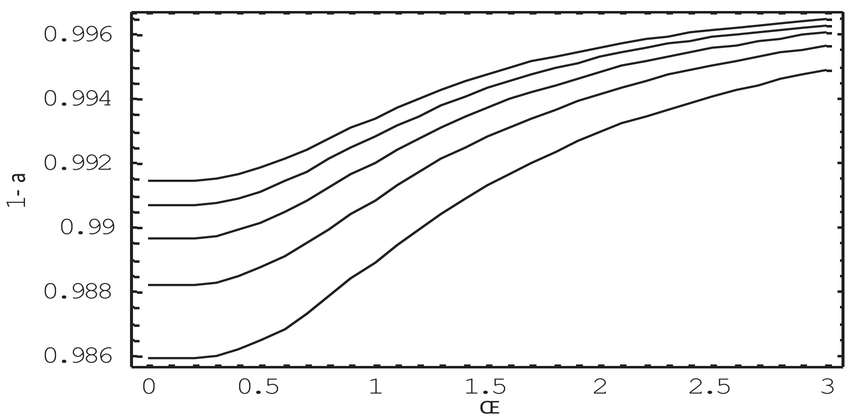

Figure 2. The sensitivity analysis for the probability of control limit vs.

Table 1. The probabilities falling into every region.

Upper Half	n=4	n=5	n=6	n=7	n=8	n=9	n=10
>3σ	0.0140849	0.0127955	0.0117962	0.0109952	0.0103361	0.0097824	0.0093096
2σ~3σ	0.0325373	0.0325160	0.0323941	0.0322281	0.0320441	0.0318547	0.0316666
1σ~2σ	0.0986155	0.1022046	0.1049198	0.1070682	0.1088238	0.1102937	0.1115482
CL~1σ	0.2607682	0.2683641	0.2740799	0.2785883	0.2822662	0.2853433	0.2879688
Lower Half	n=4	n=5	n=6	n=7	n=8	n=9	n=10
CL~1σ	0.4767506	0.4552324	0.4412385	0.4312397	0.4236533	0.4176520	0.4127561
1σ~2σ	0.1172436	0.1288874	0.1355714	0.1398804	0.1428765	0.1450394	0.1465300
2σ~3σ	0	0	0	0	0	0.0000345	0.0002206
>3σ	0	0	0	0	0	0	0

Table 2. The probabilities for each one in the Western Electronic Rules.

Upper Half	n=4	n=5	n=6	n=7	n=8	n=9	n=10
one point out	0.0140849	0.0127955	0.0117962	0.0109952	0.0103361	0.0097824	0.0093096
2 out of 3	0.0062169	0.0058803	0.0055995	0.0053625	0.0051599	0.0049844	0.0048308
4 out of 5	0.0019017	0.0020184	0.0021032	0.0021676	0.0022183	0.0022594	0.0022933
8 in a row	0.0007383	0.0008948	0.0010287	0.0011447	0.0012464	0.0013367	0.0014175
Lower Half	n=4	n=5	n=6	n=7	n=8	n=9	n=10
one point out	0.0154973	0.0135524	0.0122535	0.0113193	0.0106116	0.0100548	0.0096038
2 out of 3	0.0008340	0.0012020	0.0014601	0.0016465	0.0017859	0.0018935	0.0019786
4 out of 5	0	0	0	0	0	0	0.0000001
8 in a row	0	0	0	0	0	0	0

3. Comparison of the Control Charts

In this section, we compare the performance of the control chart we proposed with the existing control chart proposed by Spiring (1995) in terms of the operating characteristic curve and average run length (*ARL*). The operating characteristic (OC) curves are an index used to evaluate the performance of a control chart, which shows how well the control chart reacts to different degrees of changes in one process. Another index to evaluate the performance of a control chart is called *ARL*, which is the expected number of samples taken to discover a change when a process is out of control, defined as

$$ARL = \frac{1}{1-\beta}$$

To demonstrate the advantages of our proposed method, we implement the analysis of OC curves and *ARL* curves for three cases; namely, (1) the process mean μ moves to new location $\mu^* = \mu + k\sigma$, (2) the process standard deviation σ changes into a new $\sigma^* = r\sigma$, and (3) the process mean μ moves to a new location $\mu^* = \mu + k\sigma$ and the process standard deviation σ changes into $\sigma^* = r\sigma$.

Spiring (1995) developed the control chart based on the process capability index C_{pm} and derived the control limits of control chart in conjunction with X-bar and S charts, expressed as

$$P\left(\sqrt{\left(\frac{(n-1)(1+n\varepsilon^2)}{\chi^2_{n,\,n\varepsilon^2,\,1-\alpha/2}}\right)}C_{pm} \le \hat{C}_{pm} \le C_{pm}\sqrt{\left(\frac{(n-1)(1+n\varepsilon^2)}{\chi^2_{n,\,n\varepsilon^2,\,\alpha/2}}\right)}\right) \tag{6}$$

Referring to the above control limits, the OC function of the control chart based on C_{pm} for the three cases can be derived as follows, respectively.

Case 1: $\beta(C_{pm}) = P\left(\chi^2_{n,,\alpha/2} \le \chi^2_{n,\delta^*} \le \chi^2_{n,\ 1-\alpha/2}\right)$, where $\delta^* = n(\varepsilon + k)^2$.

Case 2: $\beta(C_{pm}) = P\left(\chi^2_{n,,\alpha/2} \le \chi^2_{n,\delta^*} \le \chi^2_{n,\ 1-\alpha/2}\right)$, where $\delta^* = n(\varepsilon / r)^2$

Case 3: $\beta(C_{pm}) = P\left(\chi^2_{n,,\alpha/2} \le \chi^2_{n,\delta^*} \le \chi^2_{n,\ 1-\alpha/2}\right)$, where $\delta^* = n(\varepsilon / r + k / r)^2$

According to the result of sensitivity analysis mentioned previously, ε=0 will be used to calculate the probability of β for the comparison of the two control charts.

Analysis for Case 1: when μ shifts

Table 3 displays the results of the corresponding values of β and *ARL* of the two control charts when the process mean shifts $k\sigma$ for *n*=4, 6, 8, 10, 12. From the outputs in Table 3, we can find that the performance of our proposed method is better than that of Spiring (1995) for all cases except for $k = 0$. By using our proposed method, when the process mean shifts 1.5 σ, the value β is 0.38987 and the corresponding value of *ARL* is 1.63899 for n=6. Instead, the values of β and *ARL* for Spiring (1995) are 0.64844 and 2.8445, respectively. For all sample sizes of n in Table 3, the abnormality of the process loss L_e can be quickly detected by taking less than 3 samples when the process mean shifts more than 1.5 σ. For visibility of with various $k\sigma$ shifts, the graphs of OC curves and *ARL* curves for the two control charts are depicted in Figures 3 and 4. From these graphs, we can see that both the OC curves and *ARL* curves of our proposed method are significantly steeper than those of the C_{pm} control chart, which means that the proposed method has a better sensitivity to detect the shift in process mean.

Table 3. The comparison for the performance of two control charts when the process mean shifts $k\sigma$

k	Method	n=4		n=6		n=8		n=10		n=12	
		β	*ARL*	β	*ARL*	β	*ARL*	β	*ARL*	β	*ARL*
0	The proposed	0.98592	70.9982	0.9882	84.7727	0.98966	96.7488	0.99069	107.416	0.99146	117.074
	Spiring (1995)	0.99361	156.4945	0.99254	134.0483	0.99144	116.8224	0.99030	103.0928	0.98912	91.9118
0.5	The proposed	0.96182	26.194	0.96141	25.9157	0.96044	25.2763	0.959138	24.4728	0.95763	23.6028
	Spiring (1995)	0.99361	156.4945	0.99254	134.0483	0.99144	116.8224	0.99030	103.0928	0.98912	91.9118
1	The proposed	0.83319	5.99493	0.79003	4.76252	0.74651	3.94492	0.702883	3.36568	0.65951	2.93692
	Spiring (1995)	0.95596	22.7066	0.93060	14.4092	0.90142	10.1440	0.86902	7.6348	0.83401	6.0245
1.5	The proposed	0.52651	2.11199	0.38987	1.63899	0.28108	1.39098	0.197986	1.24686	0.13664	1.15827
	Spiring (1995)	0.78659	4.6858	0.64844	2.8445	0.51309	2.0538	0.39218	1.6452	0.29104	1.4105
2	The proposed	0.19209	1.23777	0.07842	1.0851	0.02978	1.03069	0.010679	1.01079	0.00365	1.00367
	Spiring (1995)	0.44055	1.7875	0.22265	1.2864	0.10025	1.1114	0.04137	1.0432	0.01594	1.0162
2.5	The proposed	0.03397	1.03516	0.00497	1.005	0.00064	1.00064	7.49E-05	1.00007	$8.1*10^{-6}$	1.00001
	Spiring (1995)	0.13352	1.1541	0.02676	1.0275	0.00437	1.0044	0.00062	1.0006	0.00008	1.0001

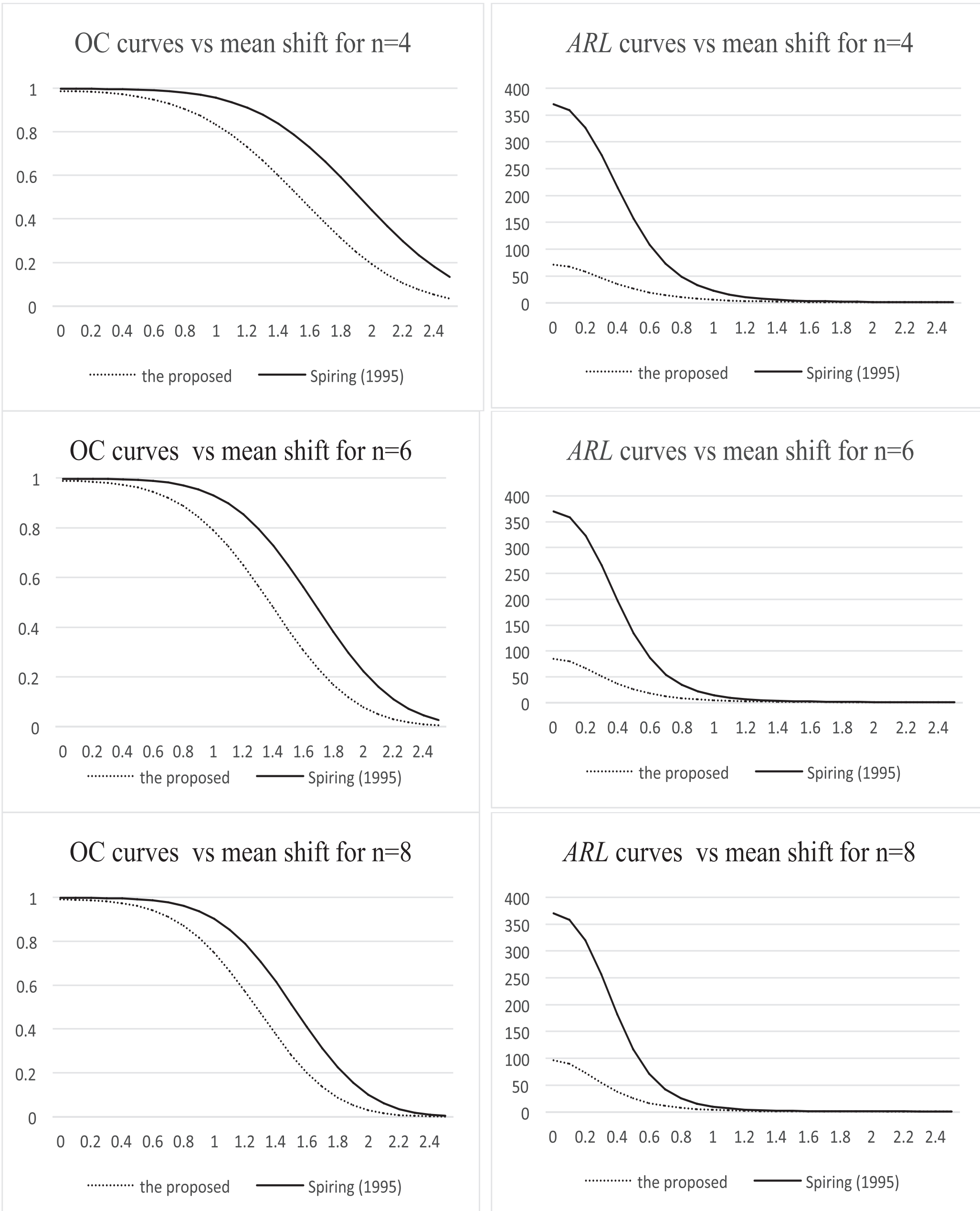

Figure 3. The β and *ARL* curves of control chart versus the $k\sigma$ shift in process mean for n=4, 6, 8.

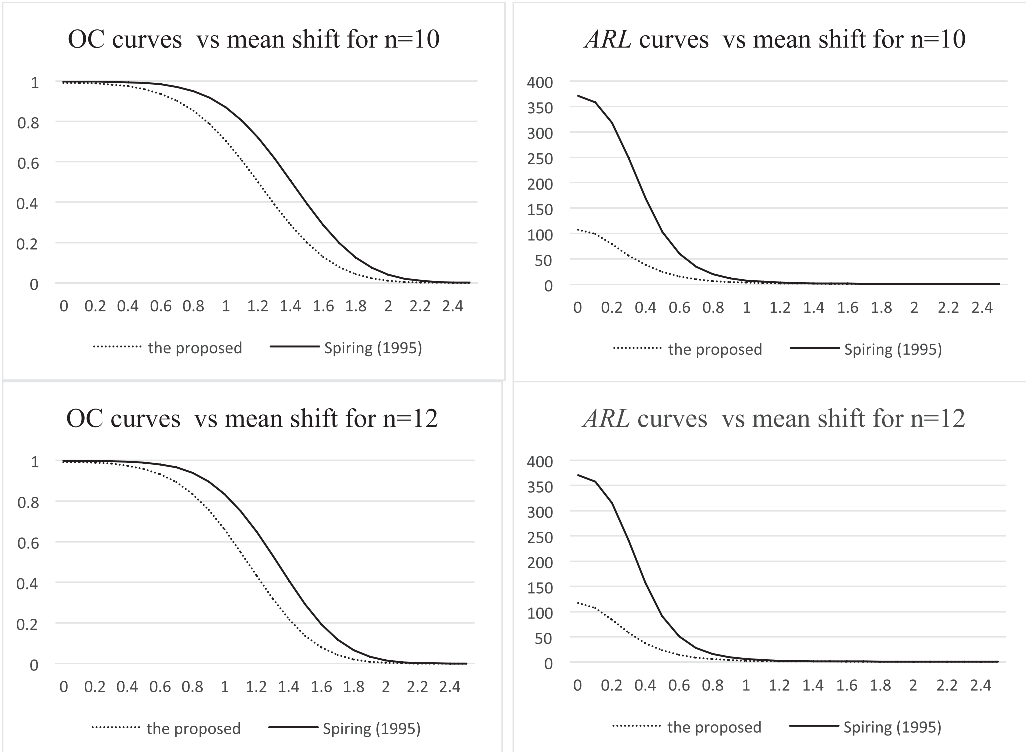

Figure 4. The β and *ARL* curves of control chart versus the $k\sigma$ shift in process mean for n=10, 12.

Analysis for Case 2: when σ changes

Table 4 displays the results of the corresponding values of β and *ARL* of the two control charts when the process standard deviation becomes $k\sigma$ for n=4, 6, 8, 10, 12. From the outputs in Table 4, we can conclude that the performance of our proposed method is better than that of Spiring (1995) for all cases except for $r = 1$. By using our proposed method, when the process changes with an expansion of 2 σ, the value of β is 0.24242 and the corresponding value of *ARL* is 1.32 for n=8. Instead, the values of β and *ARL* for Spiring (1995) are 0.39082 and 1.6416, respectively. For all sample sizes of n in Table 4, the abnormality of process loss L_e can be quickly detected by taking less than 2 samples when the expansion of process standard deviation is over 2 σ . The graphs of the OC curves and *ARL* curves for the two control charts are depicted in Figures 5 and 6. Compared with C_{pm} control chart, we can see that both the OC curves and *ARL* curves of our proposed are significantly steeper, which means that the proposed method has a better sensitivity to detect the expansion of the process standard deviation.

Table4. The comparison for the performance of two control charts when the standard deviation becomes $r\sigma$

k	Method	n=4		n=6		n=8		n=10		n=12	
		β	ARL	β	ARL	β	ARL	β	ARL	β	ARL
1	The proposed	0.98592	70.9982	0.9882	84.7727	0.98966	96.7488	0.99069	107.416	0.99146	117.074
	Spiring (1995)	0.99730	370.3704	0.99730	370.3704	0.99730	370.3704	0.99730	370.3704	0.99730	370.3704
1.5	The proposed	0.76455	4.2471	0.70475	3.38694	0.64824	2.84288	0.594485	2.466	0.54344	2.19031
	Spiring (1995)	0.90485	10.5097	0.86024	7.1551	0.81315	5.3519	0.76450	4.2463	0.71515	3.5106
2	The proposed	0.46227	1.85966	0.33659	1.50737	0.24242	1.32	0.172632	1.20865	0.12163	1.13847
	Spiring (1995)	0.65141	2.8687	0.51060	2.0433	0.39082	1.6416	0.29320	1.4148	0.21623	1.2759
2.5	The proposed	0.26381	1.35834	0.14552	1.1703	0.07881	1.08556	0.041946	1.04378	0.02198	1.02247
	Spiring (1995)	0.41640	1.7135	0.25313	1.3389	0.14812	1.1739	0.08408	1.0918	0.04654	1.0488
3	The proposed	0.15359	1.18146	0.06463	1.06909	0.02657	1.0273	0.010693	1.01081	0.00422	1.00424
	Spiring (1995)	0.26015	1.3516	0.12219	1.1392	0.05474	1.0579	0.02364	1.0242	0.00991	1.0100
3.5	The proposed	0.09313	1.10269	0.03049	1.03145	0.00972	1.00982	0.003026	1.00303	0.00092	1.00092
	Spiring (1995)	0.16507	1.1977	0.06078	1.0647	0.02122	1.0217	0.00711	1.0072	0.00231	1.0023

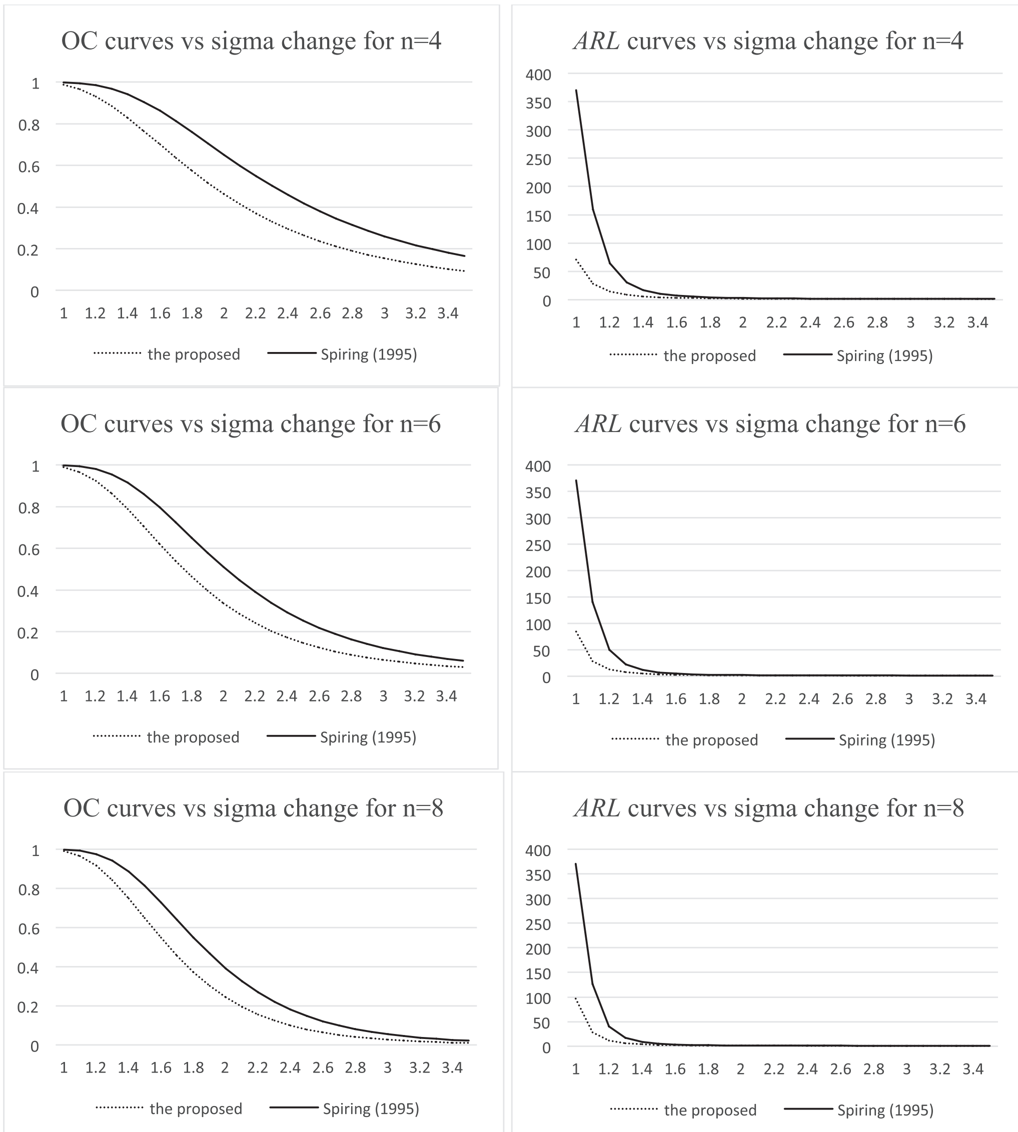

Figure 5. The β and *ARL* curves of control chart versus the $r\sigma$ variation on σ for *n*=4, 6, 8.

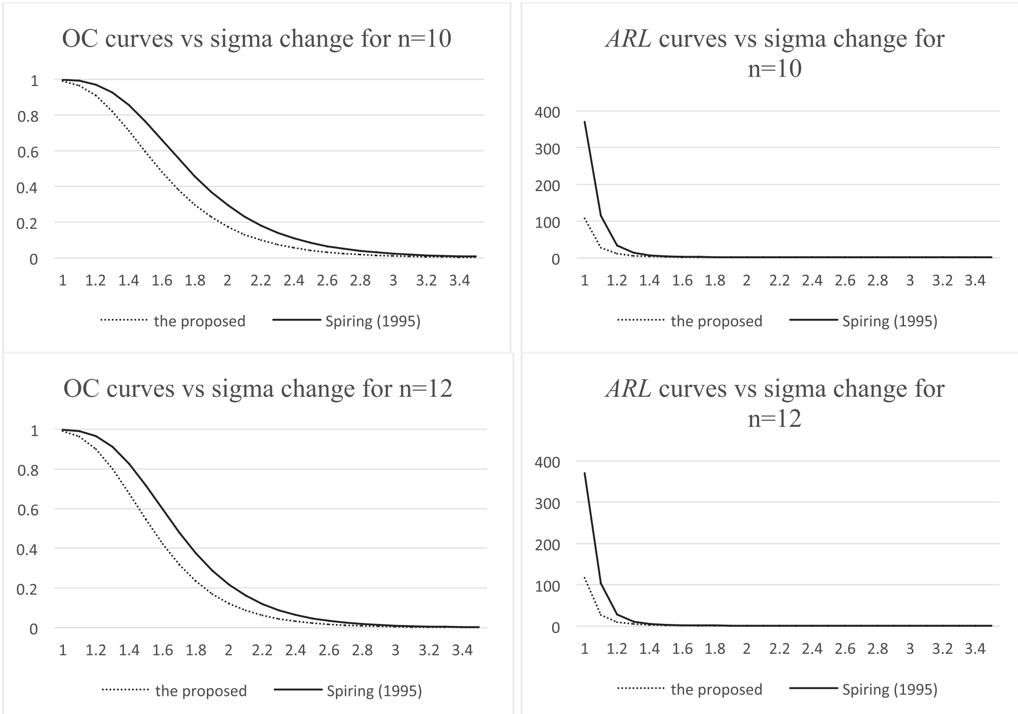

Figure 6. The β and *ARL* curves of control chart versus the $r\sigma$ variation on σ for *n*=10, 12.

Analysis for Case 3: when μ shifts and σ changes simultaneously

Table 5 displays the results of the corresponding values of β and *ARL* of the two control charts when the process mean and standard deviation change simultaneously. From the outputs in Table 5, it is obvious that the performance of our proposed method is better than that of Spiring (1995) for all cases except for $k = 0$ and $r = 1$. By using our proposed method, the value of β is 0.084723 and the corresponding value of ARL is 1.09257 with a shift in the process mean of 1σ and an expansion of the process standard deviation of 2σ given a sample size of *n*=10. Instead, the values β of and *ARL* for Spiring (1995) are 0.159334 and 1.189564, respectively. For all sample sizes of n in Table 5, the abnormality of process loss L_e can be quickly detected by taking less than 2 samples when the process mean shifts 1σ and the process standard deviation expands by 2 times. Figure 7displays the corresponding β surface plots of the two control charts with the coefficients *k* = 0.0(0.1)1.5 and *r* = 1.0(0.1)2.5 for *n*=4. From the graphs, we can observe that when the process mean shifts and process standard deviation expands simultaneously, the value β of will decrease sharply. Compared with the C_{pm} control chart, our proposed method has a better sensitivity to detect the shift of process mean and the expansion of process standard deviation.

Table 5. The comparison for the performance of two control charts when the process mean shifts $k\sigma$ and standard deviation becomes $r\sigma$

k	r	Method	n=4		n=6		n=8		n=10		n=12	
			β	ARL	β	ARL	β	ARL	β	ARL	β	ARL
0	1	The proposed	0.98592	70.9982	0.9882	84.7727	0.98966	96.7488	0.99069	107.416	0.99146	117.074
		Spiring (1995)	0.9973	370.3704	0.9973	370.3704	0.9973	370.3704	0.9973	370.3704	0.9973	370.3704
0	1.5	The proposed	0.76455	4.2471	0.70475	3.38694	0.64824	2.84288	0.594485	2.466	0.54344	2.19031
		Spiring (1995)	0.993611	156.5301	0.992541	134.0665	0.99144	116.8205	0.990301	103.1035	0.989123	91.93695
0	2	The proposed	0.46227	1.85966	0.33659	1.50737	0.24242	1.32	0.172632	1.20865	0.12163	1.13847
		Spiring (1995)	0.955959	22.70624	0.9306	14.40919	0.901415	10.14354	0.869019	7.634691	0.834011	6.024485
0	2.5	The proposed	0.26381	1.35834	0.14552	1.1703	0.07881	1.08556	0.041946	1.04378	0.02198	1.02247
		Spiring (1995)	0.786592	4.685857	0.648442	2.844481	0.513089	2.053762	0.392181	1.645226	0.291037	1.410511
0.5	1	The proposed	0.96182	26.194	0.96141	25.9157	0.96044	25.2763	0.959138	24.4728	0.95763	23.6028
		Spiring (1995)	0.904846	10.50927	0.860235	7.154849	0.813152	5.35194	0.764503	4.246346	0.715145	3.510558
0.5	1.5	The proposed	0.71172	3.46888	0.63568	2.74483	0.56579	2.30301	0.501366	2.00548	0.44228	1.79302
		Spiring (1995)	0.870524	7.723465	0.808787	5.22978	0.74505	3.922334	0.68098	3.134603	0.617975	2.617631
0.5	2	The proposed	0.43125	1.75823	0.3035	1.43575	0.21104	1.26749	0.144956	1.16953	0.09843	1.10918
		Spiring (1995)	0.758496	4.140717	0.646	2.824858	0.539848	2.173197	0.443828	1.798005	0.359734	1.56185
0.5	2.5	The proposed	0.2495	1.33244	0.13384	1.15452	0.07046	1.0758	0.036428	1.03781	0.01853	1.01888
		Spiring (1995)	0.566551	2.307079	0.398111	1.661436	0.268935	1.367868	0.176015	1.213614	0.11223	1.126418
1	1	The proposed	0.83319	5.99493	0.79003	4.76252	0.74651	3.94492	0.702883	3.36568	0.65951	2.93692
		Spiring (1995)	0.651408	2.868686	0.5106	2.043318	0.390815	1.641538	0.293196	1.414819	0.216229	1.275883
1	1.5	The proposed	0.56294	2.288	0.44988	1.8178	0.35626	1.55342	0.279442	1.38781	0.21722	1.2775
		Spiring (1995)	0.618527	2.621415	0.47043	1.888325	0.348622	1.535206	0.252816	1.338358	0.180002	1.219515
1	2	The proposed	0.34887	1.53578	0.22103	1.28374	0.13788	1.15994	0.084723	1.09257	0.05134	1.05412
		Spiring (1995)	0.526616	2.11245	0.364467	1.573482	0.244187	1.323078	0.159334	1.189534	0.101705	1.113221
1	2.5	The proposed	0.21089	1.26725	0.104	1.11607	0.05023	1.05289	0.023798	1.02438	0.01108	1.01121
		Spiring (1995)	0.396262	1.656347	0.231784	1.301718	0.129862	1.149242	0.070331	1.075652	0.037054	1.03848
1.5	1	The proposed	0.52651	2.11199	0.38987	1.63899	0.28108	1.39098	0.197986	1.24686	0.13664	1.15827
		Spiring (1995)	0.4164	1.713502	0.253132	1.338925	0.148123	1.173878	0.084076	1.091794	0.046545	1.048817
1.5	1.5	The proposed	0.36067	1.56413	0.22965	1.29811	0.14317	1.1671	0.087566	1.09597	0.05266	1.05558
		Spiring (1995)	0.397281	1.659147	0.235266	1.307645	0.133956	1.154676	0.073926	1.079827	0.039767	1.041414
1.5	2	The proposed	0.24239	1.31994	0.1278	1.14652	0.06595	1.07061	0.033364	1.03452	0.01658	1.01686
		Spiring (1995)	0.344576	1.525729	0.188474	1.232247	0.098786	1.109614	0.050066	1.052705	0.024691	1.025317
1.5	2.5	The proposed	0.15898	1.18903	0.068	1.07296	0.02841	1.02924	0.01161	1.01175	0.00466	1.00468
		Spiring (1995)	0.270687	1.371154	0.129366	1.148588	0.058921	1.062611	0.025853	1.026539	0.011009	1.011131

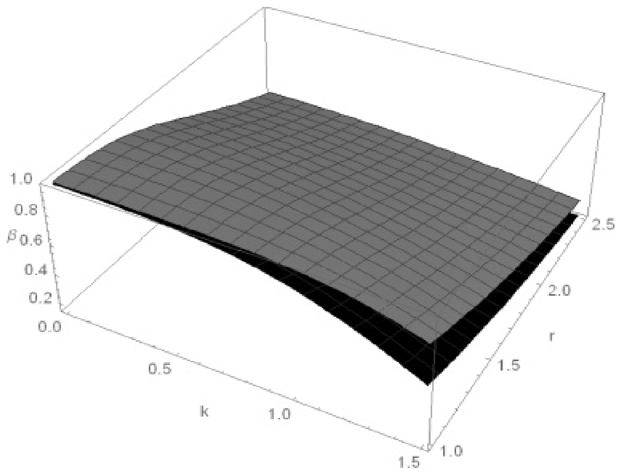

Figure 7. The OC graph of 3-sigma $\hat{L}_e$ chart versus the $r\sigma$ variation on σ and the $k\sigma$ shift in process mean for *n*=4 (the above: Spiring (1995); the bottom: the proposed method).

4. A Numerical Example

To exhibit the applicability of the proposed methodology, we present a case of color STN displays taken from Aslam et al. (2012) for illustration. Color STN (Super Twisted Nematic) displays are created by adding color filters to traditional monochrome. In color STN displays, each pixel is divided into R, G, and B sub-pixels. In this study, the membrane thickness of each pixel is the critical quality characteristic. The specification limits are *T*=12000 A^0, =12500 A^0, and =11500 A^0 ($1A^0=10^{-10}$ meter). Assume the present process obeys a normal distribution. The sample data of 25 multiple samples with a sample size of 8 are collected, shown in Table 6. Figure 8 depicts the $\overline{X}-S$ control chart for data in Table 6, which indicates that the process is in a state of control. Hence, we can make the further analysis of $\hat{L}_e$ control chart to judge if the process capability is stable. As mentioned previously, ε=0 is suggested to be used for calculating the 3-sigma control limits of $\hat{L}_e$. Based on the sample data, the mean loss $\overline{\hat{L}}_e$ from 25 subgroups, *UCL*, and *LCL* can be, respectively, calculated as

$$\overline{\hat{L}}_e = \sum_{i=1}^{25} \hat{L}_{e_i} / 25 = (0.0095+0.0118+0.0172+,\ldots\ldots,+0.0067)/25 = 0.0131,$$

$$UCL = \overline{\hat{L}}_e + 3\frac{\overline{\hat{L}}_e}{n(1+\hat{\varepsilon}^2)}\sqrt{2n+4n\hat{\varepsilon}^2} = 0.0131 + 3 * \frac{0.0131}{8(1+0)} * \sqrt{2*8+4*8*0} = 0.0328,$$

$$LCL=$$

$$Max\{0, \overline{\hat{L}}_e - 3\frac{\overline{\hat{L}}_e}{n(1+\hat{\varepsilon}^2)}\sqrt{2n+4n\hat{\varepsilon}^2}\} = Max\{0, 0.0131 - 3 * \frac{0.0131}{8(1+0)} * \sqrt{2*8+4*8*0}\} = 0.$$

The control chart of $\hat{L}_e$ is depicted in Figure 9, which shows that sample 20 is outside the upper control limit. Therefore, we can conclude that the process capability is not in a state of control.

Table 6. The data for color STN displays.

12026.29	12029.84	11982.16	12043.79	11891.35	12019.52	12020.58	11948.84
12056.84	11935.41	12068.64	12064.28	11969.27	11998.90	11987.34	11921.19
11952.76	12022.47	12116.50	12019.25	12029.93	12096.63	12014.16	12085.94
11960.73	12019.45	12033.09	12053.97	11997.11	12085.88	11985.68	12016.71
12024.08	11952.40	11898.93	12034.75	12028.32	11967.43	12010.50	12020.03
12080.60	11952.81	12061.39	12087.39	12012.18	12011.24	11994.78	11962.60
11969.07	12045.19	11980.03	12028.14	11944.20	12007.58	12065.35	11986.82
11993.49	11934.86	12033.16	12005.31	12083.07	12056.18	11943.27	11922.69
12034.84	11988.24	12011.47	11971.34	11983.51	12012.14	12037.16	12144.15
12113.39	12050.90	11995.34	12000.89	12002.38	11929.30	12050.70	12027.95
12050.30	12012.66	12075.97	11947.29	12102.62	11990.98	11909.65	12069.05
11963.68	11878.46	11968.16	11963.70	11986.12	12090.95	12094.55	12009.85
12040.96	12038.38	11929.08	11907.45	11979.25	12022.69	11955.78	11993.96
11974.91	12000.02	11986.84	12015.22	12032.42	11962.59	11896.75	12022.33
12043.70	11999.69	11976.13	11931.54	12020.84	11960.37	11985.56	12020.77
11992.62	12053.98	11892.37	12099.44	11991.81	11980.89	11964.36	11966.27
11968.00	12087.48	11991.36	11904.45	12026.44	11929.12	12103.95	11963.95
11913.92	12011.25	11925.14	11945.79	11982.36	11987.67	11980.15	11975.71
12046.97	12032.05	11991.92	12020.37	11967.17	12035.11	12089.60	12017.89
12046.75	11917.58	11808.37	11900.68	11984.35	11976.75	11958.34	12120.28
12048.01	11844.23	11956.28	11931.06	12115.21	11989.03	12035.05	11949.06
12092.65	12004.74	12041.55	11920.09	11981.61	11947.53	12009.86	12103.49
12024.94	12030.90	11991.62	12107.81	12084.82	12049.94	11964.84	12026.43
12021.88	12004.21	11998.79	11976.80	11944.83	11907.93	11998.96	11837.27
11989.92	12085.75	11983.66	12048.04	11964.44	12040.68	11977.26	12002.82

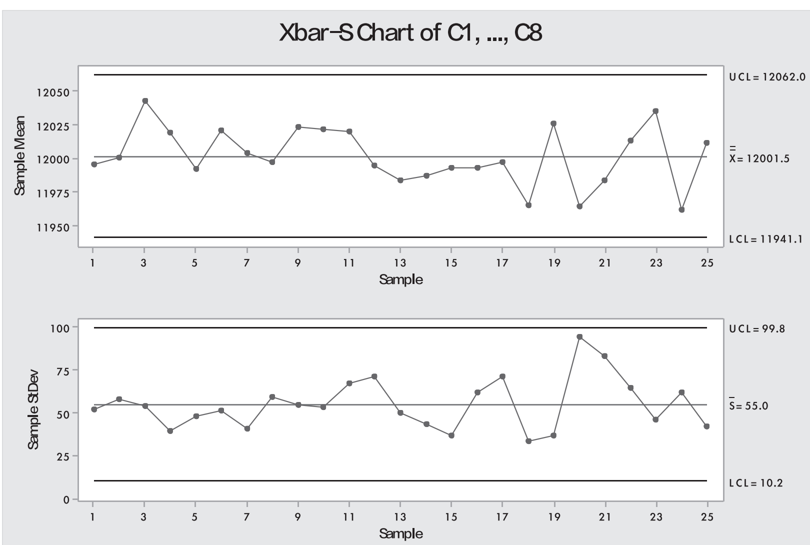

Figure 8. $\overline{X} - S$ chart for data in Table 6.

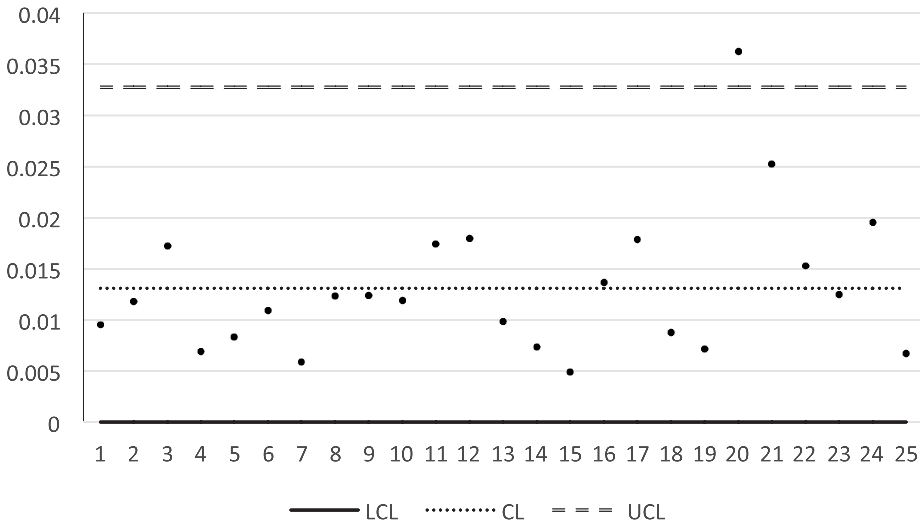

Figure 9. $\hat{L}_e$ chart for data in Table 6.

5. Conclusions

Control charts and process capability indices have been widely applied in the manufacturing industry, which are used to monitor the stability of process and measure the process capability according to the manufacturing specifications, respectively. To the best of our knowledge, no attempt has been made to propose the control chart using the process loss function. In this paper, a new control chart based on process loss index is proposed. In addition, we derive the operating characteristics function of $\hat{L}_e$ control chart and implement the analysis of β and *ARL* to compare the performance of the proposed method with that of Spiring (1995) given some specific cases. The comparisons show that the proposed method can detect the changes of process more quickly than that of Spiring (1995). By using the proposed method, practitioners can determine the sample size needed based on a desired value of the average run length to make $\hat{L}_e$ chart for monitoring the process capability.

Acknowledgements

The authors are deeply thankful to editor and reviewers for their valuable suggestions to improve the quality of this manuscript. This article was funded by the Deanship of Scientific Research (DSR) at King Abdulaziz University, Jeddah. The author, Muhammad Aslam, therefore, acknowledge with thanks, DSR technical and financial support.

References

Aslam, M., Yen, C. H., Chang, C. H., Jun, C. H., Ahmad, M. & Rasool, M. 2012. Two-stage variables acceptance sampling plans using process loss functions. Communications in Statistics-Theory and Methods, **41**(20): 3633-3647.

Chen, G., Cheng, S. W. & Xie, H. 2004. A new EWMA control chart for monitoring both location and dispersion. Quality Technology & Quantitative Management, **1**(2): 217-231.

Chen, G. & Thaga, K. 2006. A new single variable control charts: An overview. Quality and Reliability Engineering International, **22**: 811-820.

Costa, A. F. B. & Rahim, M. A. 2006. A single EWMA chart for monitoring process mean and process variance. Quality Technology & Quantitative Management, **3**(3): 295-305.

Nezhad, M. S. F. & Niaki, S. T. A. 2010. A new monitoring design for uni-variate statistical quality control charts. Information Sciences, **180**(6): 1051-1059.

Hawkins, D. M. & Deng, Q. 2009. Combined Charts for Mean and Variance Information. Journal of Quality Technology, **41**(4): 415-425.

Huang, C. C. & Chen, F. L. 2010. Economic design of max charts. Communications in Statistics—Theory and Methods, **39**(16): 2961-2976.

Johnson, T. 1992. The relationship of Cpm to squared error loss. Journal of quality technology, **24**(4), 211-215.

Khoo, M. B., Teh, S. Y. & Wu, Z. 2010a. Monitoring process mean and variability with one double EWMA chart. Communications in Statistics—Theory and Methods, **39**(20): 3678-3694.

Khoo, M. B. C., Wu, Z., Chen, C. H. & Yeong, K. W. 2010b. Using one EWMA chart to jointly monitor the process mean and variance. Computational Statistics, **25**(2): 299-316.

Li, Z., Zhang, J. & Wang, Z. 2010. Self-starting control chart for simultaneously monitoring process mean and variance. International Journal of Production Research, **48**(15): 4537-4553.

OstadsharifMemar, A. & Niaki, S. T. A. 2011. The Max EWMAMS control chart for joint monitoring of process mean and variance with individual observations. Quality and Reliability Engineering International, **27**(4): 499-514.

Ou, Y., Wu, Z. & Goh, T. N. 2011. A new SPRT chart for monitoring process mean and variance. International Journal of Production Economics, **132**(2): 303-314.

Serel, D. A. 2009. Economic design of EWMA control charts based on loss function. Mathematical and Computer Modelling, **49**(3): 745-759.

Spiring, F. A. 1995. Process capability: a total quality management tool. Total Quality Management, **6**(1): 21-34.

Spiring, F. H. & Yeung, A. S. 1998. A general class of loss functions with individual applications. Journal of Quality Technology, **30**(2): 152-162.

Teh, S. Y., Khoo, M. B. & Wu, Z. 2012. Monitoring process mean and variance with a single generally weighted moving average chart. Communications in Statistics-Theory and Methods, **41**(12): 2221-2241.

Teh, S. Y., Khoo, M. B. & Wu, Z. 2011. A sum of squares double exponentially weighted moving average chart. Computers & Industrial Engineering, **61**(4): 1173-1188.

Wu, Z. & Tian, Y. 2006. Weighted-loss-function control charts. The International Journal of Advanced Manufacturing Technology, **31**(1-2): 107-115.

Wu, Z., Wang, P. & Wang, Q. 2009. A loss function-based adaptive control chart for monitoring the process mean and variance. The International Journal of Advanced Manufacturing Technology, 40(9-10): 948-959.

Wu, Z., Tian, Y. & Zhang, S. 2005. Adjusted-loss-function charts with variable sample sizes and sampling intervals. Journal of Applied Statistics, **32**(3): 221-242.

Wu, Z. & Tian, Y. 2005. Weighted-loss-function CUSUM chart for monitoring mean and variance of a production process. International Journal of Production Research, **43**(14): 3027-3044.

Yang, S. F. 2013. Using a new VSI EWMA average loss control chart to monitor changes in the difference between the process mean and target and/or the process variability. Applied Mathematical Modelling, **37**(16): 7973-7982.

Zhang, J., Zou, C. & Wang, Z. 2010. A control chart based on likelihood ratio test for monitoring process mean and variability. Quality and Reliability Engineering International, **26**(1): 63-73.

Zhang, J., Zou, C. & Wang, Z. 2011. An adaptive Shiryaev-Roberts procedure for monitoring dispersion. Computers & Industrial Engineering, **61**(4): 1166-1172.

Zhang, S. & Wu, Z. 2006. Monitoring the process mean and variance using a weighted loss function CUSUM scheme with variable sampling intervals. IIE transactions, **38**(4): 377-387.

Zhou, Q., Luo, Y. & Wang, Z. 2010. A control chart based on likelihood ratio test for detecting patterned mean and variance shifts. Computational Statistics & Data Analysis, **54**(6): 1634-1645.

Submitted: 08/03/2016
Revised : 22/01/2017
Accepted : 16/04/2017